Supporting Information

High Performance Perovskite Solar Cells with a Non-Doped Small Molecule Hole Transporting Layer

Yang Li[1,3], Marcus D. Cole[3], Yige Gao[3], Todd Emrick[3], Zheng Xu[1], Yao Liu[2]*, and Thomas P. Russell[2,3]**

[1] Key Laboratory of Luminescence and Optical Information (Beijing Jiaotong University), Ministry of Education, Beijing, 100044, China

[2] Beijing Advanced Innovation Center for Soft Matter, Science and Engineering, Beijing University of Chemical Technology, Beijing, 100029, China

[3] Polymer Science and Engineering Department, University of Massachusetts Amherst, 120 Governors Drive, Amherst, MA 01003, USA

* Authors to whom correspondence should be addressed. Email: zhengxu@bjtu.edu.cn, liuyao@mail.buct.edu.cn, russell@mail.pse.umass.edu

Experimental Section

Materials: NPB was purchased from Xi'an Polymer Light Technology Corp. PbI_2 was purchased from Alfa Aesar. MAI was received from Dysol. $PC_{61}BM$ was received from Nano-C. PDI-Br was synthesized according to the published routes[1]. All the solvents used in this work were purchased from Sigma-Aldrich.

Device Fabrication: ITO glass substrates (20±2 Ω/sq) were purchased from Thin Film Devices Inc., and were cleaned with ultrasonic baths in detergent, deionized water, and isopropyl alcohol. All pre-cleaned ITO substrates were then dried in an oven for 6 h. Before film fabrication, the ITO substrates were treated by UV-ozone for 10 min. For the devices with PEDOT:PSS HTL, PEDOT:PSS (H.C. Starck, I 4083) was spin-coated on ITO substrates at 4000 revolutions per minute (rpm) for 40 s and annealed at 150 °C for 15 min. For the devices containing NPB HTL, NPB was dissolved in a mixture of chlorobenzene and tetrahydrofuran (1:1, volume ratio). NPB solution with different

concentrations was spin-coated on ITO substrates at 4000 rpm for 40 s inside the glove box (N_2 atmosphere, ˂1 ppm O_2, ˂1 ppm H_2O), and then annealed at 120 °C for 10 min. The film thicknesses of PEDOT:PSS and NPB were confirmed by the profilometer. After the fabrication of HTLs, the perovskite films were deposited by one-step anti-solvent method reported elsewhere[2-3], and then annealed with 10 μl *N,N*-dimethylformamide at 100 °C for 10 min. Afterwards, a 15 mg/ml $PC_{61}BM$ solution was spin-coated onto the perovskite layer at 1000 rpm for 60 s. PDI-Br in 2,2,2-trifluoroethanol (3 mg/ml) was then spin-coated onto $PC_{61}BM$ surface to serve as an interfacial modification layer. The films of perovskite, $PC_{61}BM$, and PDI-Br were all made inside a glove box (N_2 atmosphere, ˂1 ppm O_2, ˂1 ppm H_2O). Finally, an Ag electrode (100 nm) was deposited by thermal evaporation under high vacuum condition (4 ×10^{-6} mbar). The area of the solar cell was 6 mm^2 defined by metal shadow mask.

Device characterization: *J-V* characteristics were recorded using a Keithley 2400 source measurement unit under 100 mW/cm^2 (AM1.5G) irradiation using a 300 W Xe lamp solar simulator (Newport 91160). The light intensity was adjusted with an NREL-calibrated Si

reference solar cell and KG-5 filter. EIS was measured using an Agilent 4294A Precision Impedance Analyzer under 100 mw/cm^2 light intensity at 20 mv applied AC amplitude. DC bias voltage was kept at 0 V. Frequency was swept from 40 Hz to 1 MHz. Capacitance-voltage characteristics were record by Agilent 4294A under dark, frequency was fixed at 1 KHz, voltage was swept from -0.5 V to 1.5 V. All the measurements above were done inside the glove box (N_2 atmosphere, ˂1 ppm O_2, ˂1 ppm H_2O). The QE-PV-SI Measurement Kit (Newport/Oriel Instruments) with 150 W Xe arc lamp, monochromator, and calibrated silicon reference cell with power meter was used for quantum efficiency (QE)/incident photon to charge carrier efficiency measurement for solar cells over a 400-1100 nm spectral range.

Film characterization: Perovskite films were deposited on ITO/PEDOT:PSS and ITO/NPB substrates. The top-view SEM images were recorded by a FEI Magellan FESEM. A PANalytic X'Pert3 X-Ray diffractometer with a Ni filter, 1/2'' diverging slit, vertical goniometer, and X'Celerator detector was used to perform the XRD measurement, and the measurement was made from 2θ=5°-60° under Cu K-Alpha

(1.542Å). The absorption of perovskite films on different HTLs and the transmission of ITO and ITO/NPB were measured by Shimadzu UV 3600. For TRPL measurements, perovskite films were mad on glass/PEDOT:PSS and glass/NPB substrates, TRPL was recorded at the emission wavelength of 770 nm and the samples were excited at 470 nm from the glass side. Contact angles of ITO/PEDOT:PSS and ITO/NPB were measured by Dataphysics OCA 15plus, and 2 μl deionized water was used per time. Atomic force microscopy (AFM) was performed on a Digital Instruments Dimension 3100, operating in the tapping mode.

Table S1. The properties of NPB.

	HOMO (eV)	LUMO (eV)	E_g (eV)	T_g[4] (°C)	μ_h[5-8] ($cm^2V^{-1}s^{-1}$)
NPB	-5.20	-2.30	2.90	98	$(6\text{-}9)\times10^{-4}$

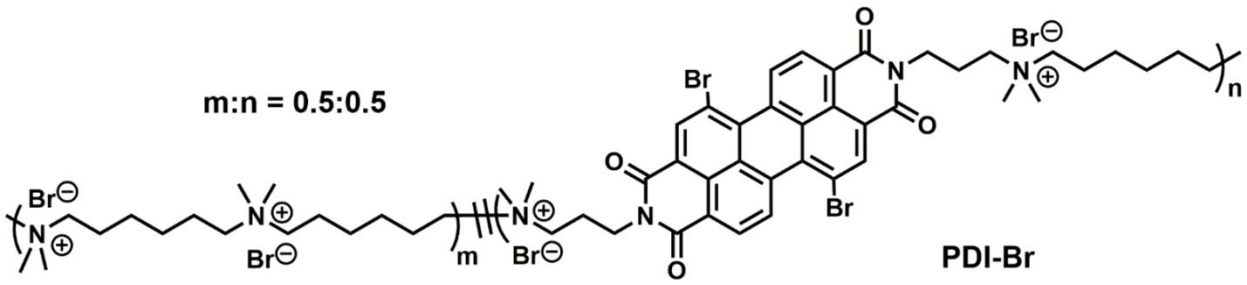

Figure S1. Chemical structure of PDI-Br interlayer.

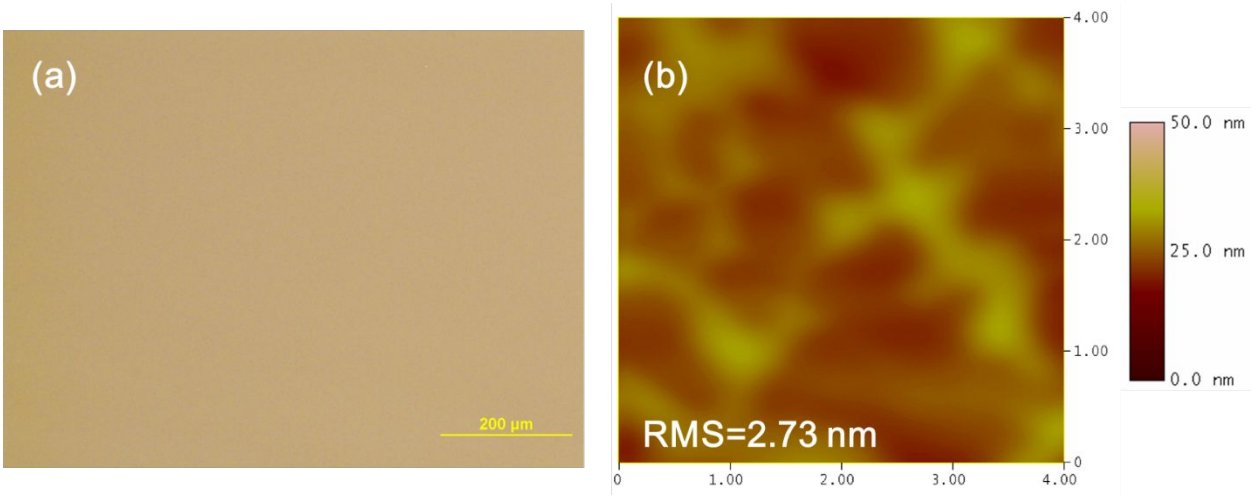

Figure S2. (a) Optical microscopy and (b) AFM images of NPB thin films (2 mg/ml) on ITO substrates. Full scale of the AFM image is 4 μm×4 μm.

Table S2. Summary of devices parameters for Figure 2a, each average value is based on 4 separate devices.

HTLs	Scan direction	J_{SC} (mA/cm^2)	V_{OC} (V)	FF (%)	PCE (%)

PEDOT:PSS	Reverse	20.49	0.97	72.3	14.35
		(19.47±0.70)	(0.95±0.027)	(72.5±2.69)	(13.44±0.64)
	Forward	19.70	0.96	73.8	14.05
NPB	Reverse	23.92	1.09	74.2	19.33
		(23.29±0.63)	(1.09±0.011)	(74.2±0.93)	(18.79±0.55)
	Forward	23.92	1.09	73.6	19.17

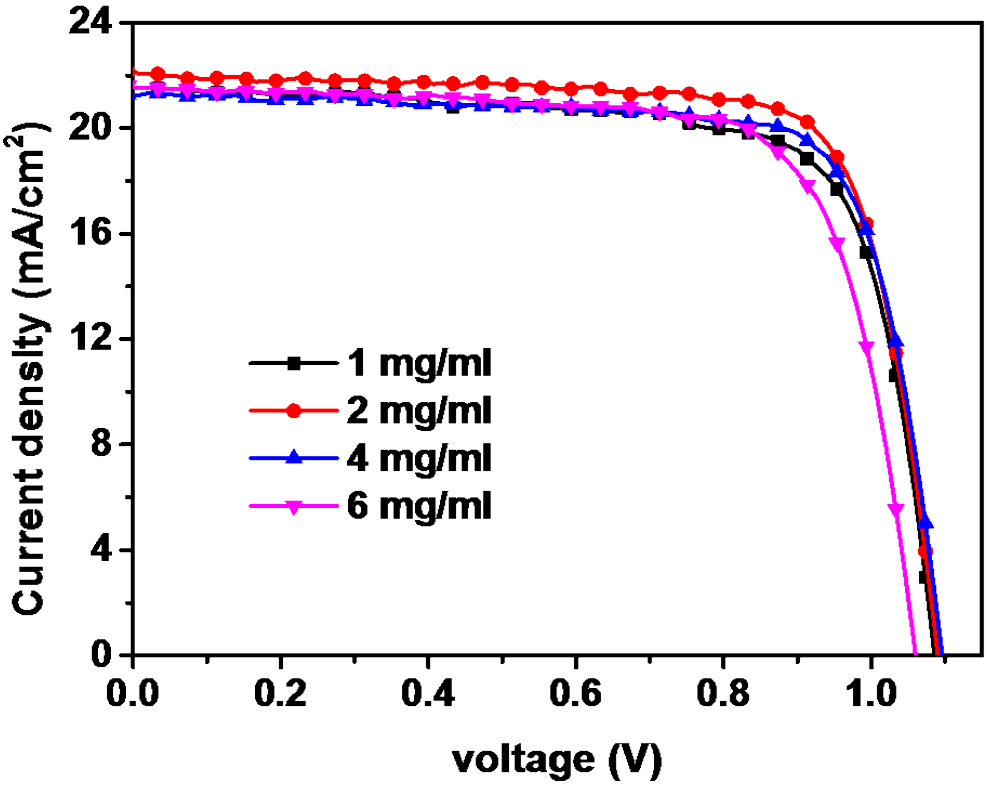

Figure S3. Current density–voltage (*J-V*) characteristics of devices based on NPB with different concentration.

Table S3. Summary of devices parameters for Figure S2, each average value is based on 5 separate devices.

NPB concentration	J_{SC} (mA/cm^2)	V_{OC} (V)	FF (%)	PCE (%)
1 mg/ml (~8 nm)	21.48	1.08	73.9	17.24
	(20.86±0.55)	(1.07±0.005)	(74.3±1.48)	(16.67±0.61)
2 mg/ml (~27 nm)	21.99	1.09	76.8	18.42
	(22.61±0.70)	(1.08±0.006)	(73.8±2.41)	(18.01±0.52)
4 mg/ml (~42 nm)	21.26	1.09	76.5	17.84
	(21.28±1.10)	(1.07±0.014)	(73.4±2.26)	(16.74±1.17)
6 mg/ml (~56 nm)	21.50	1.06	73.3	16.71
	(20.24±1.10)	(1.06±0.002)	(72.5±0.85)	(15.58±1.00)

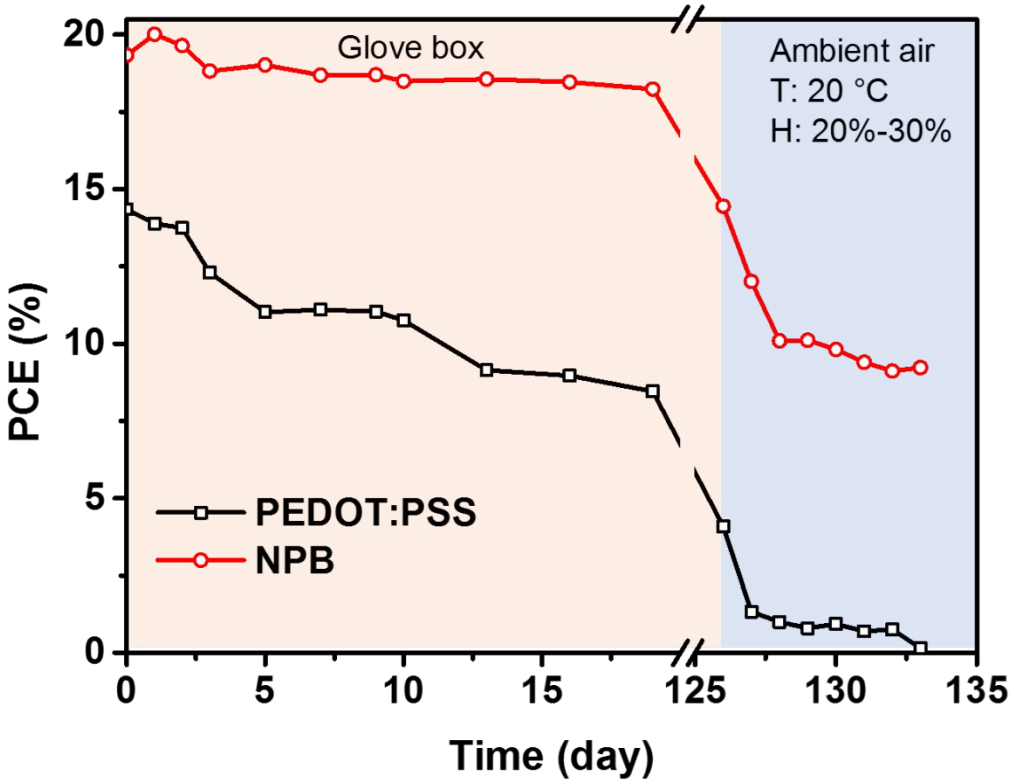

Figure S4. Stability performance of the devices in Figure 2(a).

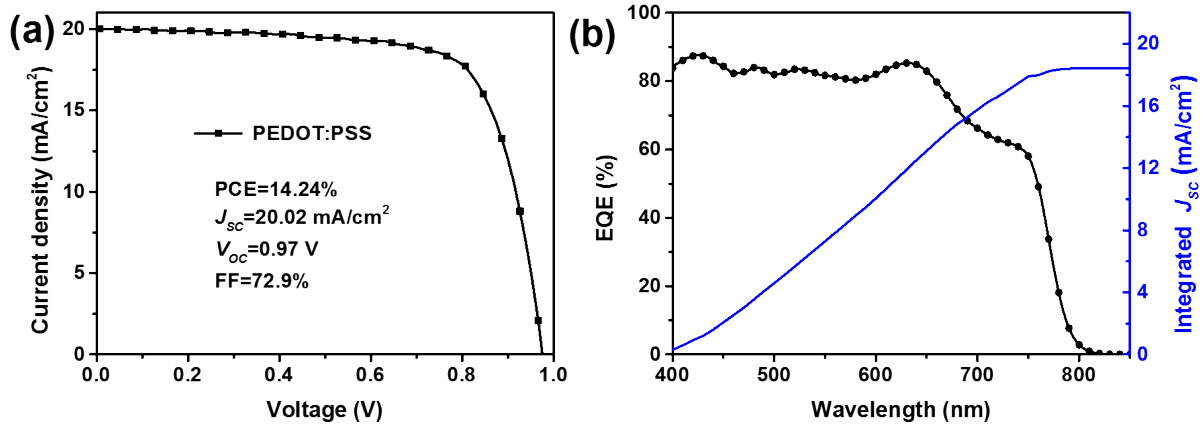

Figure S5. (a) *J-V* curve of the device with PEDOT:PSS HTL; (b) corresponding EQE profile of the device.

Table S4. J_{SC} from Figure S4 (a) and Figure 2(d), the calculated current density (J_{cal}) based on EQE from Figure S4 (b) and Figure 2(e), and the difference value (Δ) between J_{SC} and J_{cal}.

HTLs	J_{SC} (mA/cm^2)	J_{cal} (mA/cm^2)	Δ (mA/cm^2)
PEDTO:PSS	20.02	18.42	1.60
NPB	22.92	21.51	1.41

In our case, the value of J_{cal} is slightly lower than J_{SC}. The relatively low J_{cal} is mainly due to the lack of EQE profile from 300 to 400 nm, due to the limitation of our instrument. Our EQE system can only be used for the measurement over a 400-1100 nm spectral range.

Table S5. The values of FWHM at the peaks of (110), (220), and (310) in Figure 3e.

HTLs	FWHM (°)

	(110)	(220)	(310)
PEDOT:PSS	0.299	0.247	0.257
NPB	0.282	0.240	0.225

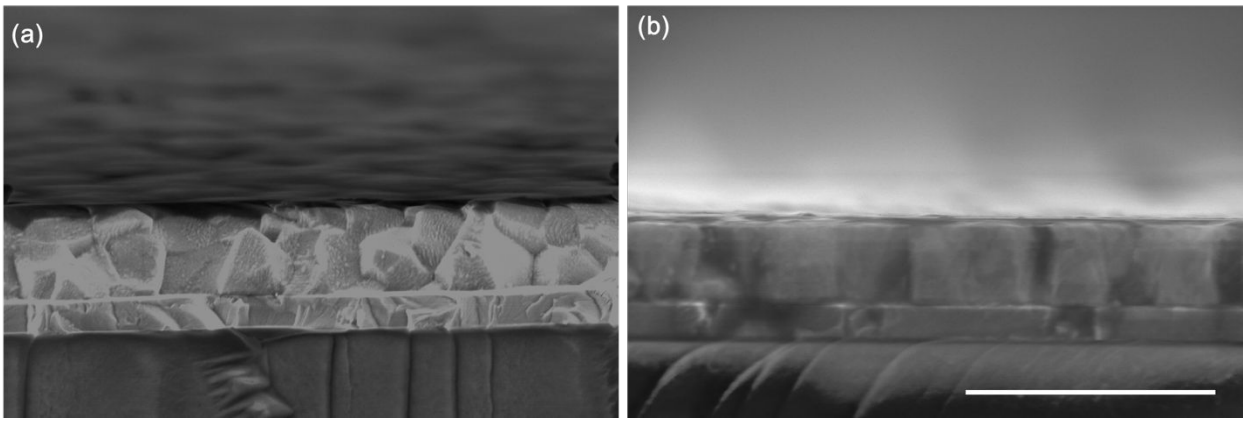

Figure S6. Cross-sectional SEM images of (a) ITO/PEDOT:PSS/perovskite/$PC_{61}BM$ and (b) ITO/NPB/perovskite/$PC_{61}BM$ (scale bar is 1 μm).

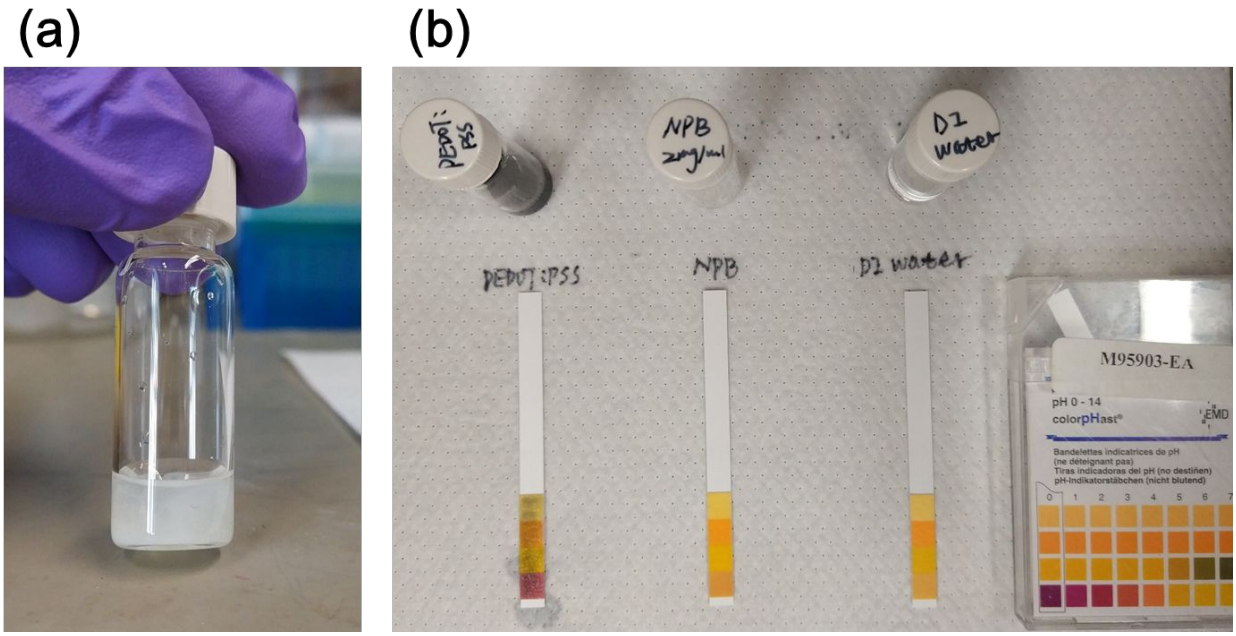

Figure S7. (a) NPB in a mixture of GBL and DMSO (1:1 vol%) (5 mg NPB in 1 ml solvent); (b) comparison of pH value between PEDOT:PSS and NPB.

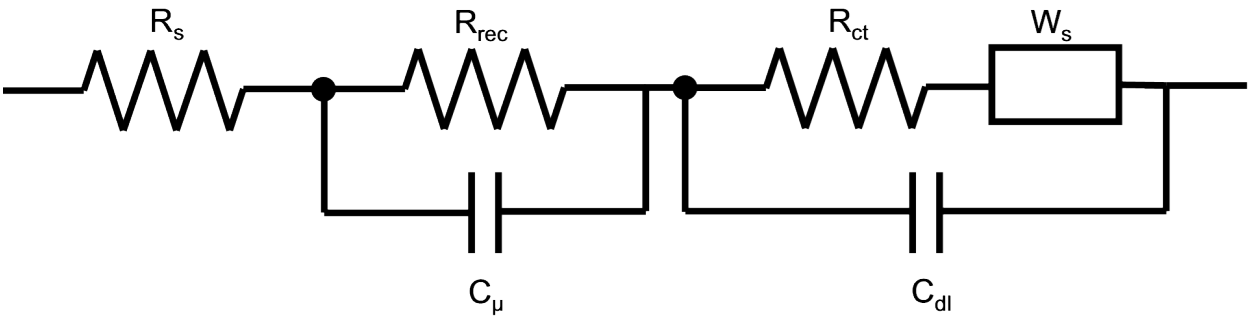

Figure S8. The equivalent circuit model for Figure 4a. This model was demonstrated based on our previous study[9-11]. Contact resistance between layers, and in the electrode contacts, is modeled with a series resistance (R_s). The high frequency impendance is modeled with charge recombination resistance (R_{rec}), while charge stored in the perovskite is modeled, in parallel, with a chemical capacitance element (C_μ). The low frequency photocapacitance was observed in our previous studies of PSCs[11], which cannot be modeled by simple interfacial capacitance. Thus, the model contains a constant phase Warburg element (W_s) modified in series with an interfacial charge transfer resistance (R_{ct}). Electronic and ionic charge accumulation at the interface is modeled with a double-layer capacitance (C_{dl}).

Table S6. EIS model fit parameters.

PSCs	R_s (Ω)	R_{rec} (Ω)	R_{ct} (Ω)
PEDOT:PSS	47	142	1032
NPB	68	1402	256

Table S7. The parameters of TRPL measurements.

HTLs	τ_1 (ns)	Fraction 1 (%)	τ_2 (ns)	Fraction 2 (%)	Averaged time (ns)
PEDOT:PSS	15.43	5.98	111.38	94.02	105.64
NPB	13.36	65.19	200.00	34.81	78.33

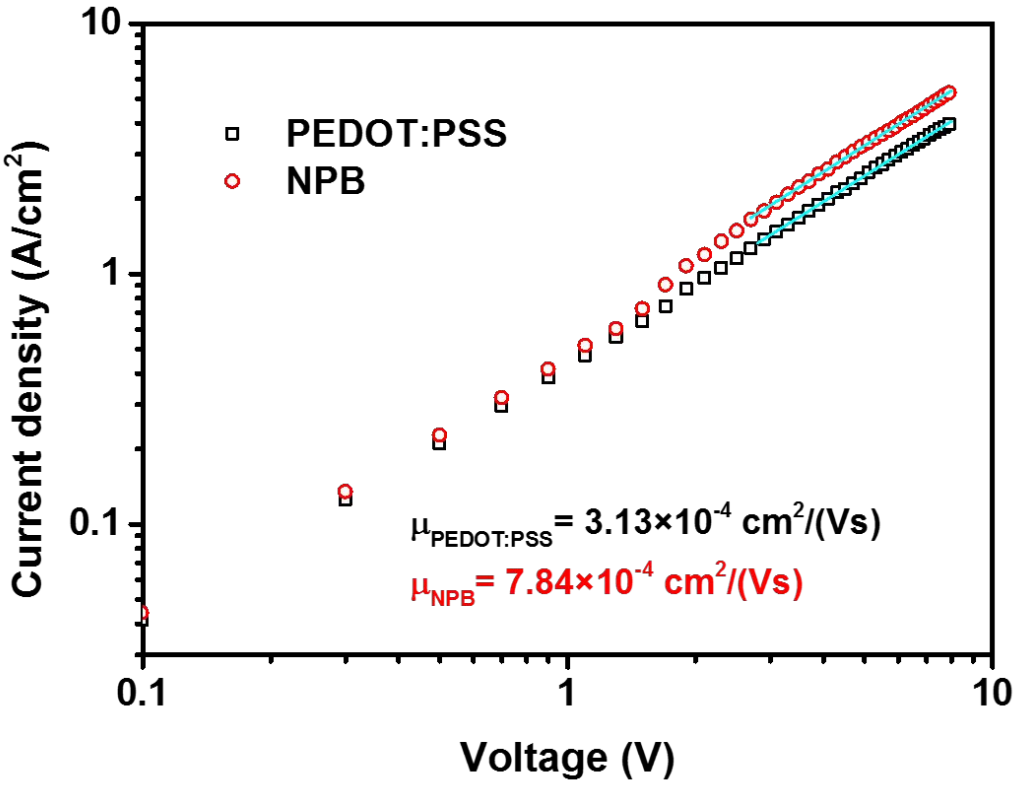

Figure S9. Hole-only devices were fabricated using the structures: ITO/PEDOT:PSS (~20 nm)/Au, and ITO/NPB (~27 nm)/Au. Hole mobility was determined by fitting the *J*-*V* curves using the Mott-Gurney relationship (space charge limited current, SCLC).

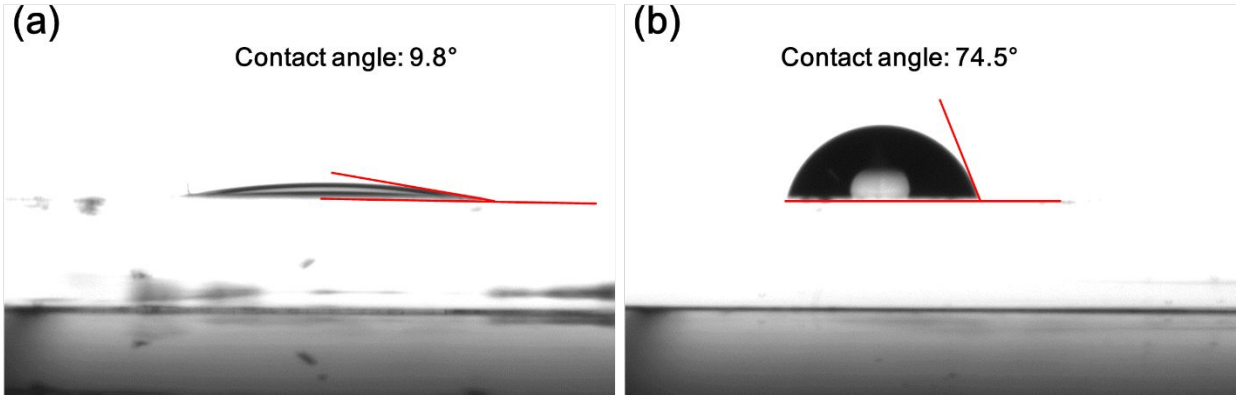

Figure S10. Contact angles of (a) ITO/PEDOT:PSS, and (b) ITO/NPB surfaces.

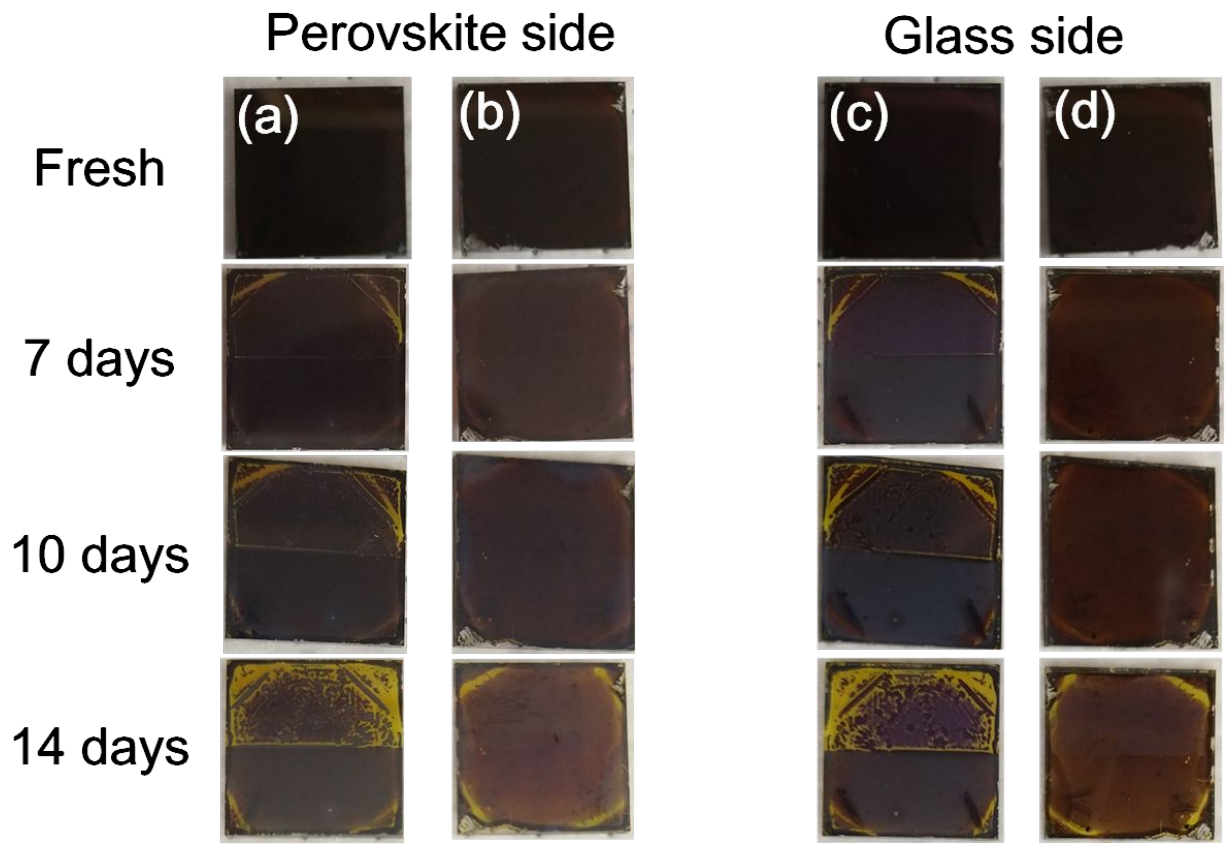

Figure S11. Photograph of the aging perovskite films based on different HTLs from perovksite side and glass side, (a) and (c) is the sample of ITO/PEDOT:PSS/$CH_3NH_3PbI_3$; (b) and (d) is the sample of ITO/NPB/$CH_3NH_3PbI_3$. The samples were stored in ambient environment with the humidity of 50-60% and the temperature of ~20 °C.

REFERENCES

(1) Cole, M. D.; Sheri, M.; Bielicki, C.; Emrick, T., Perylene Diimide-Based Ionene and Zwitterionic Polymers: Synthesis and Solution Photophysical Properties.

Macromolecules **2017**, *50*, 7535-7542.

(2) Seo, J.; Park, S.; Chan Kim, Y.; Jeon, N. J.; Noh, J. H.; Yoon, S. C.; Seok, S. I., Benefits of very Thin PCBM and LiF Layers for Solution-Processed p–i–n Perovskite Solar Cells.

Energy Environ. Sci. **2014**, *7*, 2642-2646.

(3) Li, Y.; Xu, Z.; Zhao, S.; Qiao, B.; Huang, D.; Zhao, L.; Zhao, J.; Wang, P.; Zhu, Y.; Li, X.; Liu, X.; Xu, X., Highly Efficient p-i-n Perovskite Solar Cells Utilizing Novel Low-Temperature Solution-Processed Hole Transport Materials with Linear π-Conjugated Structure. *Small* **2016**, *12*, 4902-4908.

(4) Gao, Z. Q.; Lai, W. Y.; Wong, T. C.; Lee, C. S.; Bello, I.; Lee, S. T., Organic Electroluminescent Devices by High-Temperature Processing and Crystalline Hole Transporting Layer. *Appl. Phys. Lett.* **1999**, *74*, 3269-3271.

(5) Tse, S. C.; Kwok, K. C.; So, S. K., Electron Transport in Naphthylamine-Based Organic Compounds. *Appl. Phys. Lett.* **2006**, *89*, 262102.

(6) Dong, G.; Zheng, H.; Duan, L.; Wang, L.; Qiu, Y., High-Performance Organic Optocouplers Based on a Photosensitive Interfacial C_{60}/NPB Heterojunction. *Adv. Mater.* **2009**, *21*, 2501-2504.

(7) Culligan, S. W.; Chen, A. C. A.; Wallace, J. U.; Klubek, K. P.; Tang, C. W.; Chen, S. H., Effect of Hole Mobility Through Emissive Layer on Temporal Stability of Blue Organic Light-Emitting Diodes. *Adv. Funct. Mater.* **2006**, *16*, 1481-1487.

(8) Deng, Z.; Lee, S. T.; Webb, D. P.; Chan, Y. C.; Gambling, W. A., Carrier Transport in Thin Films of Organic Electroluminescent Materials. *Synth. Met.* **1999**, *107*, 107-109.

(9) Liu, Y.; Renna, L. A.; Thompson, H. B.; Page, Z. A.; Emrick, T.; Barnes, M. D.; Bag, M.; Venkataraman, D.; Russell, T. P., Role of Ionic Functional Groups on Ion Transport at Perovskite Interfaces. *Adv. Energy Mater.* **2017**, *7*, 1701235.

(10) Bag, M.; Renna, L. A.; Jeong, S. P.; Han, X.; Cutting, C. L.; Maroudas, D.; Venkataraman, D., Evidence for Reduced Charge Recombination in Carbon Nanotube/Perovskite-Based Active Layers. *Chem. Phys. Lett.* **2016**, *662*, 35-41.

(11) Bag, M.; Renna, L. A.; Adhikari, R. Y.; Karak, S.; Liu, F.; Lahti, P. M.; Russell, T. P.; Tuominen, M. T.; Venkataraman, D., Kinetics of Ion Transport in Perovskite Active Layers and Its Implications for Active Layer Stability. *J. Am. Chem. Soc.* **2015**, *137*, 13130-13137.